

A VERSATILE ONE-POT METHOD FOR THE SYNTHESIS OF AMPHIPHILIC BIOACTIVE MAGNETIC ROSIN COATED NANOPARTICLES AS OIL SPILL COLLECTOR

A. M. ATTA^{a,b*}, H. A. AL-LOHEDAN^a, S. A. AL-HUSSAIN^{a,c}

^a*Surfactants research chair, Chemistry Department, College of Science, King Saud University, Riyadh 11541, Saudi Arabia*

^b*Egyptian Petroleum Research Institute, 1 Ahmad Elzomor St., Nasr city, 11727, Cairo, Egypt*

^c*Chemistry department, Faculty of science, Al- Imam Muhammad Bin Saud Islamic University, Riyadh 11632, Saudi Arabia*

Preparation of antimicrobial magnetic nanomaterials using cheap and bioactive materials as petroleum oil spill collector is the main goal of the present work. In this respect, magnetite was coated with different types of modified nonionic rosin surfactants in aqueous solution during formation magnetic nanoparticle at critical micelle concentrations of the rosin surfactants. The chemical structure of magnetic coated nanoparticles, morphology, thermal stability and crystal structure were investigated. The magnetic properties of the iron oxide nanoparticles were measured using VCM. The ability of the prepared magnetic nanoparticles powders to collected crude oil at the water surfaces were evaluated at different concentrations of nanomaterials. The antimicrobial activity against positive and negative grams bacterial strains was determined in the suspension. The prepared materials achieved good results approximately 95 % of oil collection at low concentration under magnetic field which was not reported elsewhere.

(Received May 10, 2015; Accepted July 3, 2015)

Keywords: Magnetite nanoparticles; Antimicrobial; crude oil collectors; Rosin; Magnetization

1. Introduction

Rosin gum or colophony is natural resin extracted from pine tree which contains more than 90 % rosin acids [1]. Chemical modifications of rosin to valuable products used in coatings, surfactants and renewable biopolymers [2-5] attracted great attention in the last decades. The applications of rosin surfactants as oil field chemicals were studied in our previous works [6-9]. The produced nonionic rosin surfactants from Diels alder adduct of rosin-maleic anhydride (R-MA) showed high dispersion efficiency for petroleum crude oil spill as nontoxic materials works [6,7]. Among several methods used to alleviate the environmental pollution produced from crude oil, chemical dispersant was used as favorable technique due to fast crude oil dispersion from water surface. This technique dispersed oil without collection. In recent work [10] magnetic fluid was used as economically feasible technique to collect more than 80 % of the petroleum crude oil spill using external magnetic field. The present work proposed technique to produce hydrophobic magnetite nanomaterials coated with rosin nonionic surfactants to apply as oil spill collector using cheap and green technique.

Magnetite nanomaterials attracted great attention in the industrial and medical applications due to unique physical and chemical properties such as their high magnetization, good biocompatibility, high thermal stability, crystallinity, etc [11-13]. There are several methods were

*Corresponding author: aatta@ksu.edu.sa

used to prepare magnetite nanoparticles such as chemical co-precipitation, sonochemical reactions, sol-gel, thermal, hydrothermal and wetting methods [14-17]. There are several disadvantages arise from these methods such as toxicity of used reagents, aggregation of magnetite, unfeasibility, oxidation of magnetite surfaces and broadness of particle sizes. We succeeded to prepare monodisperse magnetite nanoparticles with particle size between 8-11 nm using single iron salt and potassium iodide to prepare iron cations which converted at room temperature to stable magnetite in alkali solution at pH =9 using aqueous ammonia or alcoholic sodium hydroxide [18, 19]. The magnetite was coated with water soluble fraction of Myrrh gum to produce coated magnetite highly dispersed in aqueous media with high magnetization. The present work, aims to prepare highly monodisperse magnetite nanomaterials coated with nonionic rosin surfactants to prepare hydrophobic magnetite with high magnetization to easily disperse in the petroleum crude oil to use as oil spill collector in the presence of external magnetic field. The nonionic rosin surfactants were selected due to their higher efficiency to disperse crude oil [6,7] and high ability to interact with nanomaterials [20]. The measurement of antimicrobial activities of the produced magnetite powder is another goal of the present work to verify the toxicity of the produced chemicals as oil spill collectors.

2. Experimental

2.1 Materials

Rosin acid with pale yellow color [acid number = 184 mg of KOH g⁻¹, 99%] were used as commercial rosin and purified by crystallization in cold acetone. Polyethylene glycol monomethyl ether (MPEG) having molecular weights 550 and 750 g/mol, P-toluene sulfonic acid, maleic anhydride, acetic acid, anhydrous ferric chloride and potassium iodide were purchased from Aldrich Chemicals Co. The rosin maleic anhydride adduct (RMA) and their ester with MPEG were prepared according previous work [20]. The monoesters of RMA with MPEG 550 and 750 were designated as RMA-550 and RMA-750, respectively. The trimeric monomers of RMA with MPEG 550 and 750 were reported as RMA-(550)3 and RMA-(750)3, respectively.

The Arabian asphaltic heavy and paraffinic light crude oils produced by ARAMCO, Ras Tanora oil field, Saudi Arabia, were used to investigate the oil collection from the water surfaces (Arabian Gulf, Saudi Arabia).

2.2 Preparation Technique

The procedure for preparation of magnetite nanoparticles capped with rosin surfactants (RMA-550, RMA-750, RMA-(550)3 and RMA-(750)3) can be proceed as follows: anhydrous FeCl₃ (40 g) dissolved in distilled water (300 mL) and potassium iodide (13.2 g, 0.08 mol) dissolved in distilled water (50 mL) were mixed for 1h under N₂ atmosphere. Different weight of rosin surfactants were solubilized in ethanol-water solvent (100 mL, 4:1 vol%) and added dropwise to the reaction mixture (included iodine as precipitate) at the same time as 25% ammonia solution (200 mL). The reaction temperature raised up to 45 °C under continuous mixing in the presence of N₂ to form black magnetite. The precipitate was washed with ethanol after filtration and air dried without heating to produce nanomaterials.

2.3 Characterization

FTIR spectra were recorded using a Nicolet FTIR spectrophotometer (city, state abbrev if US, country) using KBr to form pellets with tested samples.

¹H-NMR and ¹³CNMR spectra of the prepared resins were recorded on a 400MHz Bruker Avance DRX-400 spectrometer.

The X-ray powder diffraction (XRD) patterns were recorded on a BDX-3300 diffractometer using CuK α radiation (wavelength, $\lambda=1.5406\text{\AA}$) with variable slits at 45 kV/40mA.

Transmission electron microscopy (TEM) micrographs were investigated with a JEOL JEM-2100F.

Dynamic light scattering (DLS) used to determine the particle size distribution. The prepared materials dispersed in ethanol/water (4/1) and model Zetasizer Nano ZS (Malvern Instruments, Malvern, U.K.) with a 633 nm He-Ne laser was used. Size distribution and zeta potential of the magnetic nanogel were estimated by a Zetasizer 3000HS PCS (Malvern Instruments)

Thermogravimetric analysis (TGA; model Shimadzu, DTG-60M) used to evaluate the thermal stability and magnetite contents at temperature range 25-850°C under N₂ atmosphere at a heating rate of 10°C min⁻¹.

The magnetic properties of the magnetite materials were evaluated using vibrating sample magnetometer (VSM; model USALDJ9600-1

The Antimicrobial activity of the prepared magnetite nanomaterials was investigated from values of minimum inhibitory concentration (MIC) and minimum bactericidal concentration (MBC) using broth-micro dilution test [19].

2.4 Evaluation of the coated magnetite/rosin surfactants as oil collector:

The efficiency of the prepared magnetite/rosin surfactants nanoparticles as oil collector as follow [19]: “The crude oil was (1 ml) spread over 250 ml of sea water. The magnetite powder was carefully added to the oil surface and stirred with 1 cm deep vortex at 200 rpm. The magnetite powder was added to the center of the vortex immediately and stirred over 60 second. The mixture was settled out for 5 min. The magnetite oil mixture was recovered using a permanent magnet of 25 mm diameter and 10 mm thickness, made with Nd-Fe-B (4300 Gauss). The remained oil was extracted using chloroform. The absorbance of extracted oil chloroform was determined against a chloroform blank at 580nm. The calibration graph of absorbance of oil/chloroform at different concentrations used to determine the concentration of oil contained in the 50cm³ oily water sample. The oil collection efficiency, OCE %, is calculated from the following equation” [19]:

$$\text{OCE \%} = \frac{\text{Weight of oil in 50cm}^3 \text{ sample of oily water} \times 500}{\text{Total weight of oil added to 250 cm}^3 \text{ separating funnel}}$$

3. Results and discussion

3.1 Chemical and crystal structure of modified magnetic/rosin surfactants

There are more than 16 iron oxides, hydroxide among of the magnetite Fe₃O₄ and maghemite Fe₂O₃ nanomaterials attracted great attention due to their academic and industrial importance. The present work proposed new method to prepare coated magnetite nanoparticles using modified biomaterials such as nonionic rosin surfactants. It was previously reported that the drawback of the aqueous phase syntheses is that the variation of the molar ratios between ferrous and ferric salts used to prepare magnetite, moreover the aggregations and low oxidation stability of magnetite which overcome with high thermal method techniques that used high energy and ferric organic salts [11]. Taking in the consideration these limitations, the present work represented new method to produce monodisperse and stabilized magnetite nanoparticles at room temperature using aqueous phase precipitation of one iron salt in the presence of KI and ammonia solution [10, 21]. This versatile method was used for production of both bare and surface-coated magnetite nanoparticles. Furthermore, the proposed method presents a “greener” and more sustainable pathway to prepare amphiphilic magnetite nanoparticles that can easily be scaled up to produce large, commercially relevant quantities of both bare and surface modified iron oxide nanoparticles. We selected here magnetite nanoparticles to use as oil spill collector. The magnetite was prepared

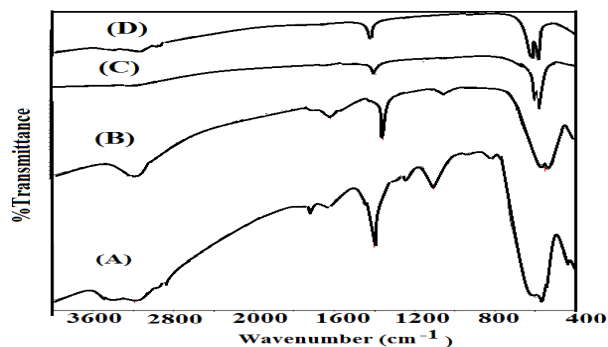


Fig. 1: FTIR spectra of A) $Fe_3O_4/RMA-550$, B) $Fe_3O_4/(RMA-550)_3$, C) $Fe_3O_4/RMA-750$ and D) $Fe_3O_4/RMA-(750)_3$.

The crystalline structure and the identification type of iron oxide can be confirmed by XRD analysis. In this respect, The XRD diffractograms of RMA-550 and RMA-(750)₃ were selected as representative samples and interpenetrated in Figure 2. All diffractograms showed the same patterns that can be related to the magnetite phase in accordance with the JCPDS powder diffraction document [PDF No. 65-3107]. All diffractograms showed broad diffraction peaks which corresponded to small nanosizes and small crystallites.

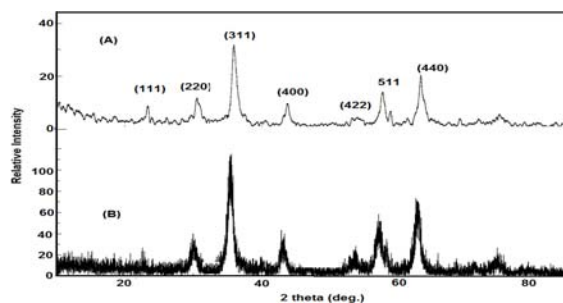


Fig.2: XRD diffractograms of A) $Fe_3O_4/RMA-550$ and B) $Fe_3O_4/RMA-(750)_3$.

Thermal analyses such as thermogravimetric (TGA) and differential thermal (DTA) are very important technique used to determine the percentage of metal nanomaterials coated with organic materials and types of metal oxide conversion. In this respect, both TGA and DTA curves of magnetite coated with nonionic rosin surfactants were selected and represented in Fig. 3A-D. DTA curves showed different exothermic peaks at 165, 350-450, 630 and 750-900 °C. There are two peaks appeared without weight loss which appeared at 165 and 650°C. These peaks represented the transformation of Fe_3O_4 to $\gamma-Fe_2O_3$ and to $\alpha-Fe_2O_3$, [22]. The possible explanation to disappearance of peak at 165 °C can be referred to the presence of coats on magnetite limits the conversion. The DTA analyses, fig. 3 A-D, indicated that the high binding between magnetite and rosin surfactants except that coated with RMA-550 and RMA-750 surfactants. TGA curves, Fig. 3 A-D, indicated that the weight loss of rosin surfactants increased from 250 to 450 °C. These curves indicated that the residue at 600 °C which represent the contents of magnetite were 84, 86, 80 and 82 % for RMA-550, RMA-(550)₃, RMA-750 and RMA-(750)₃, respectively. The TGA residue for normal magnetite was 95.23% as reported in previous work [10, 21]. These data indicated that the magnetite content decreased with increasing the molecular weight of MEG due to coiling and increased with increasing the MPEG content due to steric stabilization of magnetite nanoparticle with increasing of MPEG contents [23]. The weight loss region between 250 and 450 °C was correlated with exothermic DTA peaks in these regions which indicated that approximately 12-16 % of rosin surfactants were used to coat magnetite. The residual at 900 °C was used to estimate the

α -Fe₂O₃ contents as were 68, 74, 54 and 68 % for RMA-550, RMA-(550)3, RMA-750 and RMA-(750)3, respectively. These results indicated that the magnetite were efficiently coated with nonionic rosin surfactants and the magnetite has higher oxidation stability when coated with RMA-550, RMA-(550)3 surfactants.

3.2 Morphology and particle size distribution:

The morphology of the magnetite coated with RMA-550, RMA-(550)3, RMA-750 and RMA-(750)3 is very important to determine the different types of interactions among magnetite, rosin coats, and magnetite/coat molecules. In this respect TEM micrographs were detected and represented in Fig. 4A-D. Careful inspection indicated that magnetite/RMA-550 and magnetite/RMA-(750)3 formed aggregates and clusters, respectively. While, magnetite/RMA-(550)3 and magnetite/RMA-750 formed dispersed nanoparticles. In our previous work [20], it was determined that the silica nanoparticles were interacted more with branched surfactants based on RMA-(750)3 and the adsorption of surfactant was increased. It was suggested the MPEG branches acted as bridge between silica and facilitate the adsorption at the solid surfaces. It was also reported that the adsorption was altered by hydrophobicity of silica. In the present work, it can be observed from TEM data, Fig 4. A-D, that increasing the molecular weight of MPEG from 550 to 750 g/mol will increase the hydrophilicity of the rosin surfactants and decreased the hydrophobic interaction between hydrophenancerene of rosin group(Scheme 1) that enhance the dispersability of magnetite in aqueous solution.

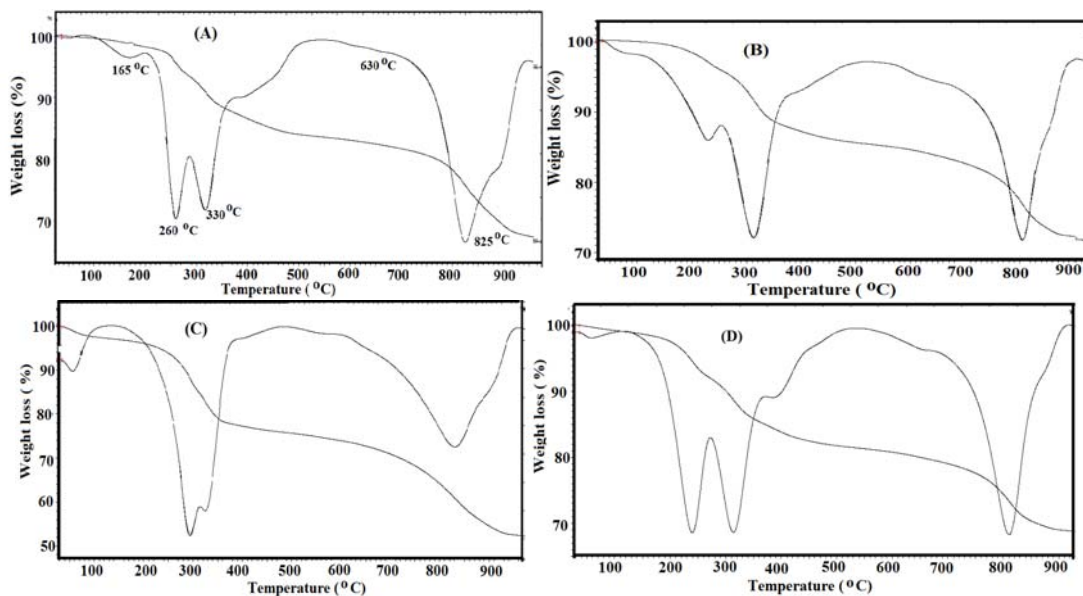


Figure 3: TGA thermograms of A) Fe_3O_4 /RMA-550, B) Fe_3O_4 /(RMA-550)3, C) Fe_3O_4 /RMA-750 and D) Fe_3O_4 /RMA-(750)3.

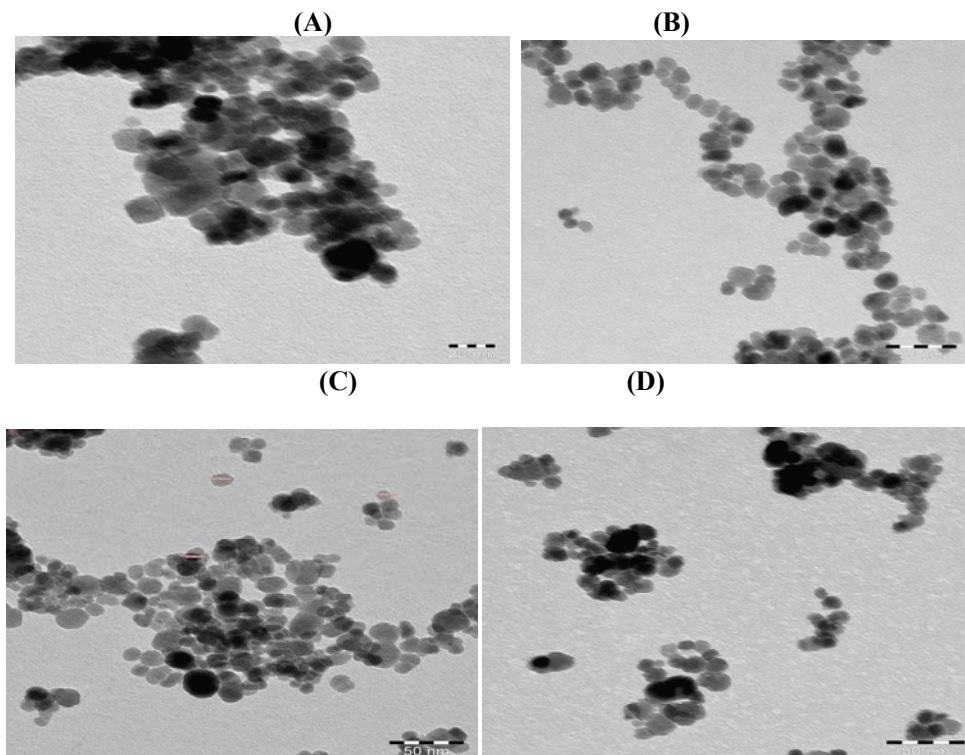


Fig. 4: TEM micrographs of A) $Fe_3O_4/RMA-550$, B) $Fe_3O_4/(RMA-550)_3$, C) $Fe_3O_4/RMA-750$ and D) $Fe_3O_4/RMA-(750)_3$.

The coiling of MPEG 550 in water due to low molecular weight leads to formation of aggregates when interact with magnetite. It was also observed that the increment of MPEG molecular weight and branches, RMA-(750)₃, increase the interaction with magnetite and lead to rotate the hydrophobic group of rosin to water which increased the hydrophobic interaction and consequently lead to formation of cluster (Fig. 4 D).

DLS measurements were used to determine the particle size and their distribution. Zeta potential was used to estimate the particle charges and stability of particles dispersions. The DLS analysis of magnetite coated with RMA-550, RMA-(550)₃, RMA-750 and RMA-(750)₃ were determined and represented in Fig.5.A-D. Their DLS and zeta potentials data were listed in Table 1.

The data of DLS measurements indicated the formation of monodisperse magnetite nanoparticles when coated with RMA-(550)₃ and RMA-750 with particle size ranged from 11-14 nm. Moreover, the magnetite formed aggregates (10-25 nm) and clusters from 10 up to 45 nm when the surface was coated with RMA-550, and RMA-(750)₃. The data of DLS agree in harmony with the data of TEM (Fig.4). The zeta potentials of the dispersed particles were all positive at neutral condition pH=7. It was determined that the magnetite coated with RMA-750 showed good stability than others against aggregation [24-26]. The formation of rosin surfactants shell was indicated by the change of zeta potential uncoated magnetite nanoparticles from nearly zero to +45.5 mV. It can be concluded that the coated magnetite nanoparticles having small size, particles size distribution and high charges are less likely to aggregate or form clusters.

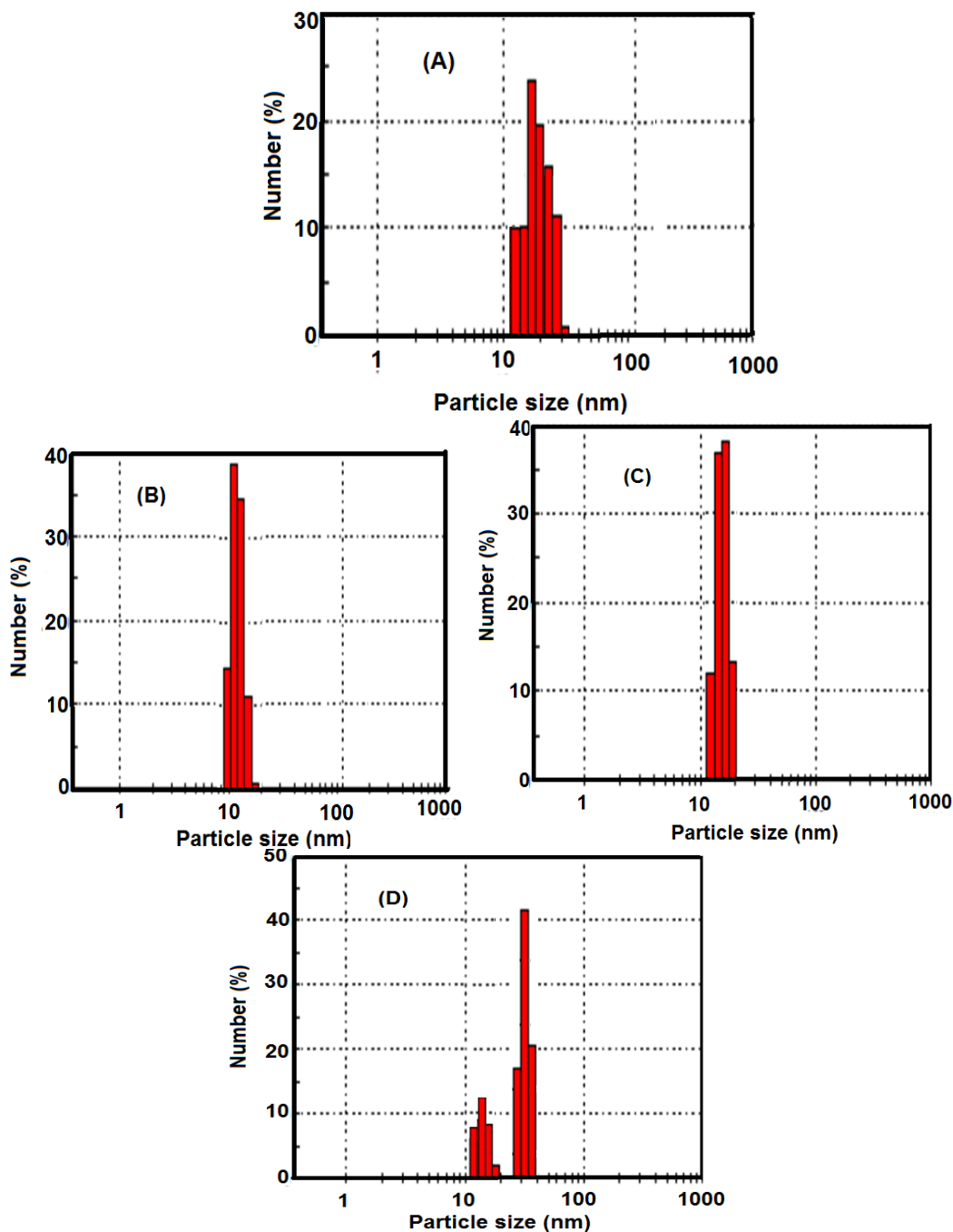


Fig. 5. DLS data of A) $Fe_3O_4/RMA-550$, B) $Fe_3O_4/(RMA-550)_3$, C) $Fe_3O_4/RMA-750$ and D) $Fe_3O_4/RMA-(750)_3$

3.3 Magnetization and application

Magnetic parameters such as saturation magnetization (M_s), coercivity (H_c) and remnant magnetization (M_r) are important characteristics to determine the magnetization of the magnetic materials. These parameters were determined from the magnetization hysteresis curves, which represented for magnetite nanoparticles coated with RMA-550, RMA-(550)₃, RMA-750 and RMA-(750)₃ surfactants and represented in Fig. 6. The values of M_s , H_c and M_r were listed in

Table 2. The magnetic materials showed a superparamagnetic behavior, no remanence magnetism was observed when the magnetic field was removed at room temperature. For the RMA-750 coated magnetite particles, the M_s value is 62.95 emu g^{-1} which is the highest value found to be about 70% of the magnetization given for magnetite in the literature (89 emu g^{-1} magnetite) [27,28]. The lower values of M_s than that of the bulk materials was normal for nanoparticles. This was referred to interaction between the magnetite atoms surfaces with surfactant to create a magnetically dead layer [29-31]. The high M_s value of magnetite coated with RMA-750 and RMA-(550)3 was attributed to good crystallinity nature of magnetite as confirmed by XRD. Moreover, very little remanence effects (M_r) indicated the quasi-superparamagnetic property of magnetite coated with RMA-750 and RMA-(550) [32]. The strong magnetization of magnetite nanoparticles coated with RMA-550, RMA-(550)3, RMA-750 and RMA-(750)3 suggests its applicability for collection of petroleum crude oil using magnetic separation technique.

Table1: . The DLS and Zeta Potential measurements of the samples.

Sample	DLS (nm)	Zeta Potential (mV)
$\text{Fe}_3\text{O}_4/\text{RMA-550}$	27 ± 17	25.83 ± 0.60
$\text{Fe}_3\text{O}_4/\text{RMA-(550)3}$	12 ± 3	45.53 ± 0.70
$\text{Fe}_3\text{O}_4/\text{RMA-750}$	15 ± 3	38.89 ± 0.65
$\text{Fe}_3\text{O}_4/\text{RMA-(750)3}$	45 ± 15	16.93 ± 0.42

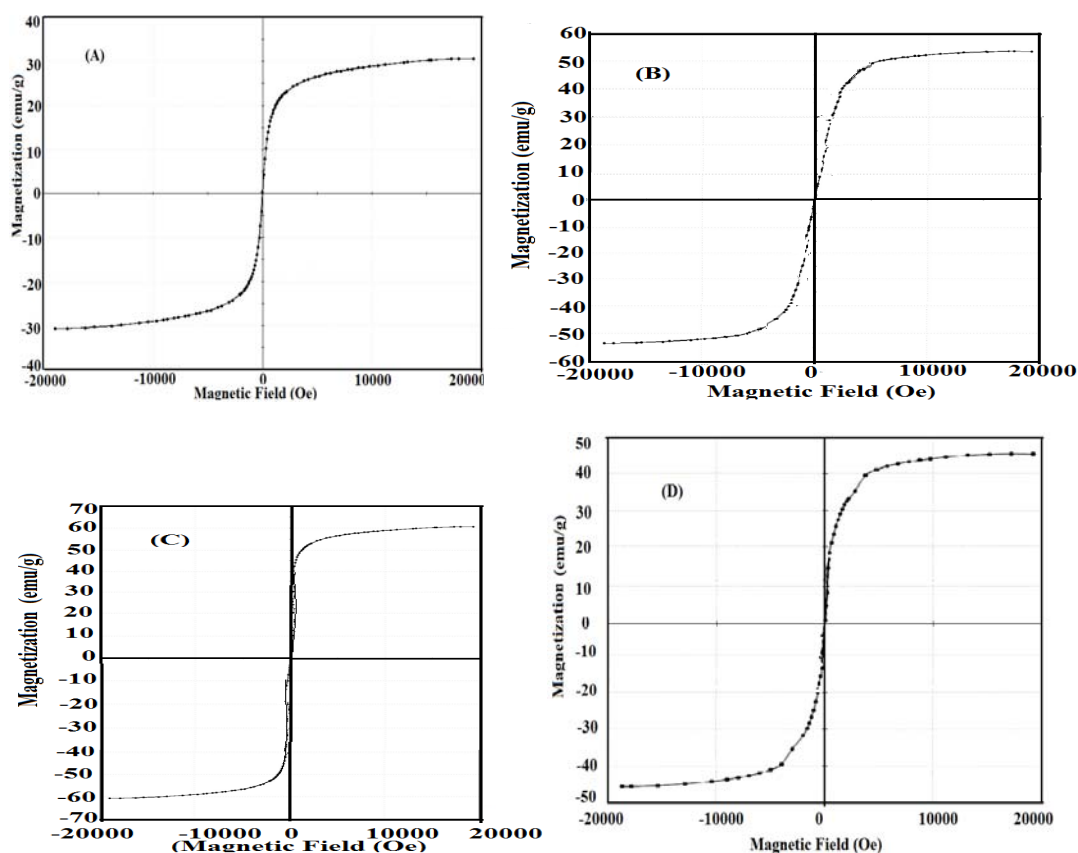


Fig. 6: VSM curves of A) $\text{Fe}_3\text{O}_4/\text{RMA-550}$, B) $\text{Fe}_3\text{O}_4/(\text{RMA-550})_3$, C) $\text{Fe}_3\text{O}_4/\text{RMA-750}$ and D) $\text{Fe}_3\text{O}_4/\text{RMA-(750)3}$.

Table 2: Magnetic characteristics of magnetite nanoparticles.

Samples	Ms (emu/g)	Mr (emu/g)	Hc (G)
Fe ₃ O ₄ / RMA-550	33.41	19.4	9.25
Fe ₃ O ₄ / RMA-(550)3	50.1	7.4	5.38
Fe ₃ O ₄ / RMA-750	62.95	6.97	5.13
Fe ₃ O ₄ / RMA-(750)3	44	14.95	5.37

The application of magnetite powder coated with RMA-550, RMA-(550)3, RMA-750 and RMA-(750)3 surfactants was evaluated as represented in the experimental section. Two different types of crude oil based on heavy and light were used for this purpose to study the effect of crude oil chemical constituent on the oil collection efficiency (OCE %). Different magnetite to oil ratios (MOR) were used to determine the best effective ratio can be used to collect the petroleum crude oil spill. The values of OCE % were measured at different MOR at 25 °C and listed in Table 3. The data indicated that the magnetite powders have the same behaviors at high magnetite content MOR (1/1) in both light paraffinic and heavy asphaltic crude oils. The magnetite powder coated with RMA-750 and RMA-(550)3 achieved good results at low concentration MOR (1/20). This result agrees in harmony with the DLS, zeta potential and magnetization data which indicated that these materials have good dispersion stability and super-paramagnetization behavior. The asphaltic crude (heavy) achieved good results for OCE % that paraffinic (light) crude due to the presence of asphaltene in asphaltic crude which can adsorb at magnetite surfaces to increase the stability of magnetite/rosin surfactants in the crude and decrease any possibility to disperse in sea water.

3.4 Antimicrobial activity

The antimicrobial activity of magnetite coated rosin surfactants should be tested due to the presence of lot numbers of various bacterial species in sea water that can degrade the rosin surfactants and precipitate the magnetite which affects their dispersability in crude oil. Moreover, the toxicity of chemicals to microorganism should be evaluated for any chemical dispersed in water due to ecological rules. The materials should be safe to the marine environment. This section addresses the antimicrobial activity of nonionic rosin surfactants doped magnetite nanoparticles at in vitro level as described in the experimental section. The minimum inhibitory concentration (MIC; $\mu\text{g mL}^{-1}$) of magnetite coated nanoparticles using different types of gram positive (*Staphylococcus aureus* ATCC 6538 and *Bacillus subtilis* ATCC 6633) and negative (*Escherichia coli* ATCC 8739 and *Pseudomonas aeruginosa* ATCC 10145) bacterial strains were determined and listed in Table 4. The data indicated that Fe₃O₄/ RMA-(750)3 and Fe₃O₄/ RMA-750 achieved good results with all tested bacterial strains. The MIC values were ranged from 2.5 to 10 $\mu\text{g mL}^{-1}$ that completely inhibited the growth of *S. aureus* and *B. subtilis*.

Table 3: OCE % of magnetite nanomaterials coated with nonionic rosin surfactants.

Samples	MOR		OCE %	
	magnetite	Oil	heavy	Light
Fe ₃ O ₄ / RMA-550	1	1	92	86
	1	10	77	84
	1	20	68	80
Fe ₃ O ₄ / RMA-(550)3	1	1	93	92
	1	10	92	85
	1	20	97	90
Fe ₃ O ₄ / RMA-750	1	1	90	92
	1	10	92	92
	1	20	95	93
Fe ₃ O ₄ / RMA-(750)3	1	1	97	96
	1	10	92	89
	1	20	77	84

The bacterial growth by magnetite was referred to the superoxide and hydroxide radicals of Fe₃O₄, resulted from an oxidative stress; act as the causative agent of such damage and consequent affect to proteins, membranes and DNA [33]. It was expected that the nuclei of bacilli in the sample culture will rupture due to interaction with the magnetic nanoparticles. In the present work, the bond between ether group of MPEG and superoxide radical of Fe₃O₄ enhanced antimicrobial activity of the resultant nanoparticles and completely inhibited as MIC was achieved. This finding agrees in harmony with other studies which proved that iron oxide nanoparticles substantially inhibited the growth of *E. coli* and *S. aureus* at concentrations comparative to that used in our work [34, 35]. Finally, we can concluded that the presence of slightly high molecular weight and content of MPEG of nonionic rosin surfactants at magnetite nanoparticle surface increases the antimicrobial activity of magnetite nanoparticles due to their ability to adsorb at interfaces and forming biofilms at the nanoparticle surfaces [36, 20].

Table 4. Minimum inhibition concentration (MIC) and the % reduction of organism for 10, 5, 2.5, and 1 mg mL⁻¹ of samples against *Escherichia coli* ATCC 8739, *Staphylococcus aureus* ATCC 6538, *Bacillus subtilis* ATCC 6633, *Pseudomonas aeruginosa* ATCC 10145 strains.

Antimicrobial materials	Types Organism	MIC $\mu\text{g mL}^{-1}$	The reduction of organism (%)			
			1 $\mu\text{g mL}^{-1}$	2.5 $\mu\text{g mL}^{-1}$	5 $\mu\text{g mL}^{-1}$	10 $\mu\text{g mL}^{-1}$
Fe ₃ O ₄ /RMA-550	<i>E. coli</i>	>10	50±3	52±5	54±7	78±2
	<i>S. aureus</i>	-	-	-	56±4	58±9
Fe ₃ O ₄ /RMA-(550)3	<i>E. coli</i>	10	-	25±4	52±7	80±8
	<i>S. aureus</i>	10	-	-	65±7	85±4
Fe ₃ O ₄ /RMA-750	<i>E. coli</i>	>10	37±10	47±5	49±4	71±1
	<i>S. aureus</i>	>10	29±3	36±3	42±4	62±2
	<i>B. subtilis</i>	2.5	36±3	92±3	95±3	97±2
	<i>P. aeruginosa</i>	>10	30±2	32±4	39±5	56±8
Fe ₃ O ₄ /RMA-(750)3	<i>E. coli</i>	10	44±6	61±2	77±5	83±7
	<i>S. aureus</i>	5	34±3	39±4	92±4	97±2
	<i>B. subtilis</i>	2.5	64±7	95±3	96±2	97±2
	<i>P. aeruginosa</i>	10	64±5	86±4	87±4	89±5

4. Conclusions

Monodisperse stable dispersed magnetite nanoparticles were produced after coating magnetite with nonionic rosin surfactants RMA-750 and RMA-(550)3 with particle size ranged from 11-14 nm. DLS measurements indicate that the coated magnetite nanoparticles of rosin surfactants shell possess small size, particles size distribution and high charges (zeta potential +45.5 mV) and they are less likely to aggregate or form clusters. The high magnetization value and very little remanence effects of magnetite coated with RMA-750 and RMA-(550)3 was attributed to good crystallinity nature the quasi-superparamagnetic property of magnetite as confirmed by XRD and VSM. The magnetite powder coated with RMA-750 and RMA-(550)3 achieved good results for oil spill collection under magnetic field at low concentration MOR (1/20). Magnetite nanoparticles inhibited on a certain range of concentrations the ability of gram positive (*Staphylococcus aureus* ATCC 6538 and *Bacillus subtilis* ATCC 6633) and negative (*Escherichia coli* ATCC 8739 and *Pseudomonas aeruginosa* ATCC 10145) to grow in suspension. The results demonstrating their potential use in the design of antibacterial oil spill collector and exhibiting also the great advantage of reduced cytotoxicity on eukaryotic host cells and tissues in the our forthcoming publication.

Acknowledgments

The project was financially supported by King Saud University, Vice Deanship of Research Chairs.

References

- [1] S. Maiti, S. Das, M. Maiti, A. Ray, In *Polymer Application of Renewable-Resource Materials*; Carraher, C. E., Sperling, L. H., Eds.; Plenum Press: New York, p 129 (1983).
- [2] S. Maiti, S. S. Ray, Kundu, A. K. *Progress of Polymer. Science*, **14**, 297 (1989).
- [3] A. M. Atta, R. Mansour, *Journal of Polymer Research*, **12**, 127 (2005).
- [4] A. M. Atta, H. M. Bedawy, I. F. Nassar, *Reactive and functional polymers*, **67**, 617 (2007).
- [5] Y. Zheng, K. Yao, J. Lee, D. Chandler, J. Wang, C. Wang, F. Chu, C. Tang, *Macromolecules*, **43**, 5922 (2010).
- [6] A. M. Atta, M. E. Abdel-Rauf, N. E. Maysour, A. K. Gafer, *Journal Dispersion Science Technologies*, **31**, 583 (2010).
- [7] A. M. Atta, A. M. Elsaed, *Journal of Applied Polymer Science*, **122**, 183 (2011).
- [8] A. M. Atta, G. A. El-Mahdy, H. S. Ismail, H. A. Al-Lohedan, *International Journal Electrochemical Science*, **7**, 11834 (2012).
- [9] A. M. Atta, G. A. El-Mahdy, H. A. Al-Lohedan, S. A. Al-Hussain, *International Journal of Molecular Science*, **15**, 6974 (2014).
- [10] A. M. Atta, A. K-F. Dyab, EP 2804 186 A1, November (2014).
- [11] C. W. Jung, P. Jacobs, *Magnetic Resonance Imaging*, **13**, 661 (1995).
- [12] J. Liu, S. Z. Qiao, Q. H. Hu, G. Q. Lu, *Small*, **7**, 425 (2011).
- [13] J. Chomoucka, J. Drbohlavova, D. Huska, V. Adam, R. Kizek, J. Hubalek, *Pharmacological Research*, **62**, 144 (2010).
- [14] C. E. Astete, C. S.S.R. Kumarb, C. M. Sabliov, *Colloids and Surfaces A: Physicochemical Engineering Aspects*, **299**, 209 (2007).
- [15] S. Laurent, D. Forge, M. Port, A. Roch, C. Robic, L. V. Elst, R. N. Muller *Chemical Reviews*, **108**, 2064 (2008).
- [16] V. Yathindranath, L. Rebbouh, D. F. Moore, D. W. Miller, J. V. Lierop, T. Hegmann, *Search Results, Advanced Functional Materials*, **21**, 1457 (2011).
- [17] P. A. Dresco, V. S. Zaitsev, R. J. Gambino, B. Chu, *Langmuir*, **15**, 1945 (1999).
- [18] A-H. Lu, E. L. Salabas, F. Schuth, *Angewandte Chemie International Edition*, **46**, 1222 (2007).
- [19] A.M. Atta, H.A. Al-Lohedan, S. A. Al-Hussain, *International Journal of Molecular Science*, **16**(4), 6911-6931 (2015).
- [20] A. M. Atta, H. A. Al-Lohedan, *Journal Surfactants & Detergents*, **05/10.1007/s11743-014-1589-y** (2014).
- [21] A.M. Atta, H.A. Al-Lohedan, S. A. Al-Hussain, *Molecules*, **19**, 11263 (2014).
- [22] B. Tural, N. O'zkan, M. Volkan, *Journal Physical Chemistry of Solids*, **70**, 860 (2009).
- [23] R. Matsuno, K. Yamamoto, H. Otsuka, A. Takahara. *Macromolecules*, **37**, 2203 (2004).
- [24] J. Hong, P. Gong, D. Xu, H. Sun, S. Yao, *Journal of Applied Polymer Science*, **105**, 1882 (2007).
- [25] K. M. Ho, P. Li, *Langmuir*, **24**, 1801-1807 (2008).
- [26] H. Suna, Yua, J.; Gongga, P.; Xua, D.; Zhanga, C.; Yao, S. *Journal of Magnetism and Magnetic Materials*, **294**, 273 (2005).
- [27] L. P. Ramirez, K. Landfester, *Macromolecular Chemistry and Physics*, **204**, 22 (2003).
- [28] N. A. D. Burke, H. D. H. Stover, F. P. Dawson, *Chemistry of Materials*, **14**, 4752 (2002).
- [29] M. F. Zhang, S. G. Shi, J. X. Meng, X. Q. Wang, H. Fan, Y. C. Zhu, X. Y. Wang, Y. T. Qian, *Journal of Physical Chemistry*, **112**, 2825 (2008).
- [30] Wang, X.; Wang, L.; He, X.; Zhang, Y.; Chen, L. *Talanta*, **78**, 327 (2009).
- [31] Z. Xu, C. Li, X. Kang, D. Yang, P. Yang, Z. Hou, J. Lin, *Journal of Physical Chemistry C*, **114**, 16343 (2010).

- [32] J. Zhou, L. Meng, X. Feng, X. Zhang, Q. Lu, *Angewandte Chemie*, **122**, 8654 (2010).
- [33] T. Gordon, B. Perlstein, O. Houbara, I. Felner, E. Banin, S. Margel, *Colloids and Surfaces A*, **374**, 1 (2011).
- [34] A. Prodan, S. L. Iconaru, C. M. Chifiriuc, C. Bleotu, C. S. Ciobanu, M. Heino, S. Sizaret, D. J. Predoi, *Nanomaterials*, **2013**, Article ID 893970, 7 pages (2013).
- [35] C. Chiiriuc, V. Laz˘ar, C. Bleotu, *Digest Journal of Nanomaterials and Biostructures* **6**, 37 (2011).
- [36] W. C. Miles, P. P. Huffstetler, J.D. Goff, A. Y. Chen, J. S. Riffle, R. M. Davis, *Langmuir*, **27**, 5456 (2011).